

## **SUPPLEMENTARY MATERIAL**

### **Systematic study of high field strength elements during liquid immiscibility between carbonatitic melt and silicate melt**

**Wanzhu Zhang<sup>1</sup>, Shuo Xue<sup>2,3\*</sup>, Ming-Xing Ling<sup>1\*</sup>, Xing Ding<sup>4</sup>**

<sup>1</sup> State Key Laboratory of Nuclear Resources and Environment, East China University of Technology,  
Nanchang 330013, China

<sup>2</sup>CAS Key Laboratory of Mineralogy and Metallogeny, Guangzhou Institute of Geochemistry, Chinese  
Academy of Sciences, Guangzhou 510640, China

<sup>3</sup> CAS Center for Excellence in Deep Earth Science, Guangzhou 510640, China

<sup>4</sup> State Key Laboratory of Isotope Geochemistry, Guangzhou Institute of Geochemistry, Chinese  
Academy of Sciences, Guangzhou 510640, China.

---

\* Corresponding author. E-mail address: xueshuo@gig.ac.cn

\* Corresponding author. E-mail address: mxling@ecut.edu.cn

## Contents of this file

Text S1. Electron microprobe analysis

Text S2. LA–ICP–MS analysis

Figure S1-S7

## Additional Supporting Information (Files uploaded separately)

Captions for Tables S1 to S3

## Introduction

- Text S1-S2 provides detailed description of EPMA analysis and LA–ICP–MS analysis.
- Figure S1-S4 include the HFSE content characteristics of natural carbonatite samples, the correlation diagram between SiO<sub>2</sub> content and HFSE contents in carbonatite and silicate melts and the correlation diagram between  $D_{HFSE}^{CM/SL}$  and F and SO<sub>3</sub> in carbonatitic melt. Figure S5. Comparison of partition coefficients of high field strength elements between carbonatite and conjugate alkaline silicate melts from this study and previous studies. Figure S6. Diagrams illustrating the dependence of  $D_{Si}^{CM/SL}$  on pressure and temperature.

## Text S1. Electron microprobe analysis

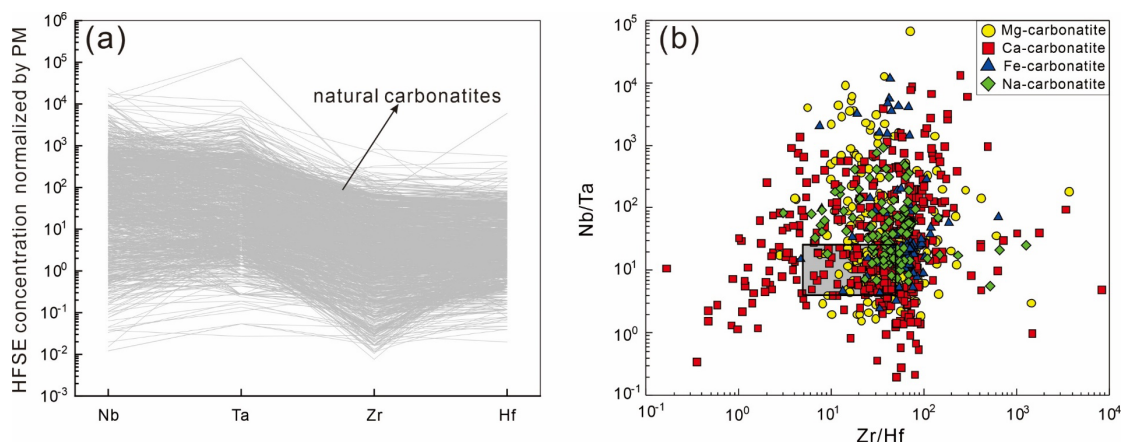
The experiment run products were mounted in resin and then polished using ethanol to avoid dissolving carbonate phases. The JEOL JXA-8230 EPMA, equipped with WDS and BSE imaging, was used to analyze the phase assemblages and textures of the quenched silicate and carbonatitic melts. The quenched silicate and carbonatitic melts were subjected to analytical conditions that included a 15 kV acceleration voltage, a 10 nA beam current, and a 20 μm diameter beam size. The peak counting time was 10 s for Na, 20 s for Si, Ca, Al, Mg, and F. To obtain accurate concentrations of S in the

quenched silicate glasses and carbonatitic melts, a peak counting time of 180 s and analytical conditions of 15 kV and 70 nA were used. The instrument was calibrated using natural and synthetic standards, such as albite for Na, chrome-diopside for Si and Ca, olivine for Mg, spinel for Al, fluoride for F, and barite for SO<sub>3</sub>. BCR-2G anhydrous basaltic glasses were used to monitor the accuracy of major elements (Jochum and Nohl, 2008), and NIST 610 was used to monitor the accuracy of S (Jochum et al., 2011). The analytical accuracy was estimated to be better than 2% relative for SiO<sub>2</sub>, Al<sub>2</sub>O<sub>3</sub>, and CaO, 5% relative for MgO, and 10% relative for Na<sub>2</sub>O, SO<sub>3</sub>, and F. The CO<sub>2</sub> content in the carbonated silicate melts was estimated using EPMA analytical totals from 100 wt.% with the method previously described in previous studies (Dasgupta and Hirschmann, 2006; Lane and Dalton, 1994).

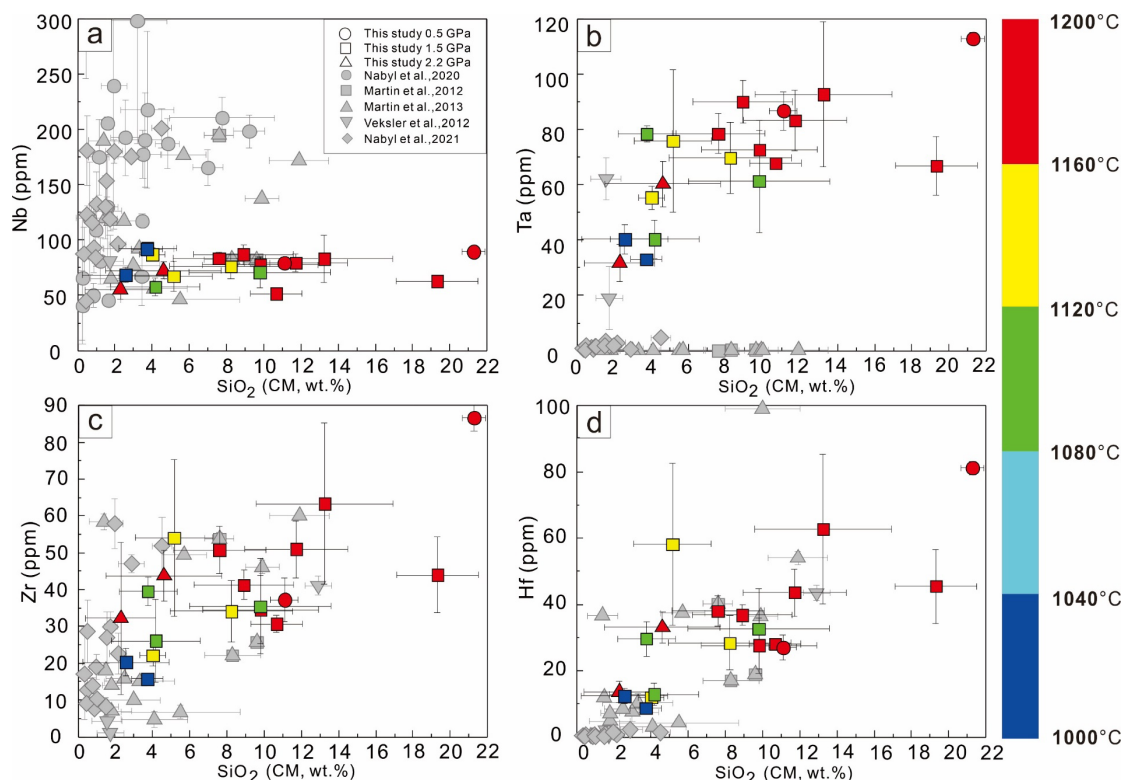
#### **Text S2. LA-ICP-MS analysis**

The silicate and carbonatitic melts were subjected to Laser Ablation-Inductively Coupled Plasma-Mass Spectrometry (LA-ICP-MS) analysis to determine their major and trace element compositions. The analysis was carried out using a Photon Machines Analyte HE 193 nm ArF Excimer Laser Ablation system coupled to an Agilent 7900 Quadrupole ICP-MS. The laser was operated at a frequency of 8 Hz and an energy of approximately 2 J/cm<sup>2</sup> for 40 seconds, preceded by a 20-second measurement of a gas blank. The laser beam size ranged from 40 to 70 μm. Helium was used as a carrier gas, mixed with argon as the make-up gas via a T-connector before entering the ICP. Dwell times of 10 ms were used for isotopes <sup>23</sup>Na, <sup>25</sup>Mg, <sup>27</sup>Al, <sup>29</sup>Si, <sup>31</sup>P, <sup>39</sup>K, <sup>43</sup>Ca, <sup>91</sup>Zr, <sup>93</sup>Nb, <sup>178</sup>Hf and <sup>181</sup>Ta. Quantification of all elements was carried out using the NIST 610 standard glass, with additional checks made using the NIST 612 and BCR-2G natural basaltic glass standards (Pearce et al., 1997; Rocholl, 1998), all analyzed under the same ablation conditions as the samples. Ca and Si contents determined by EPMA were used as internal standards for carbonatitic and silicate melts, respectively. Data processing was performed offline using ICPMSDataCal (Liu et al., 2008). The estimated analytical uncertainties due to internal and external standardization were approximately 5% for major elements and 10-15% for trace elements.

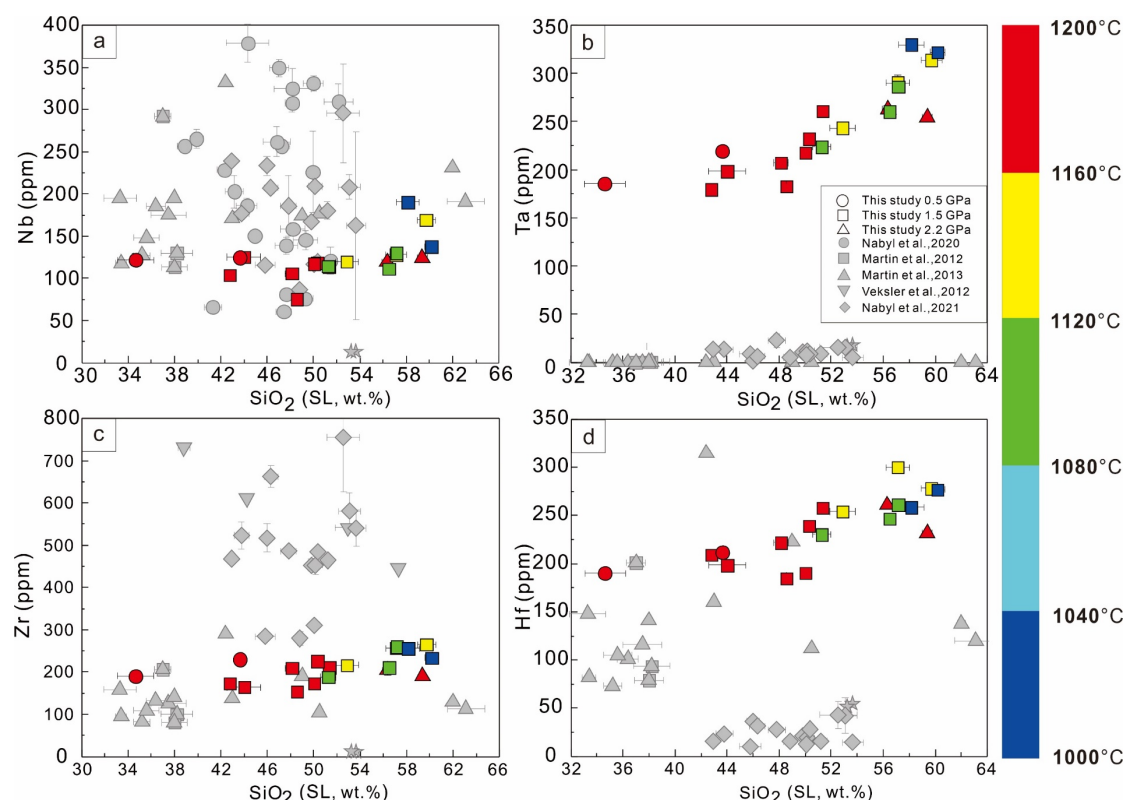
## Supplementary Figure S1-S7



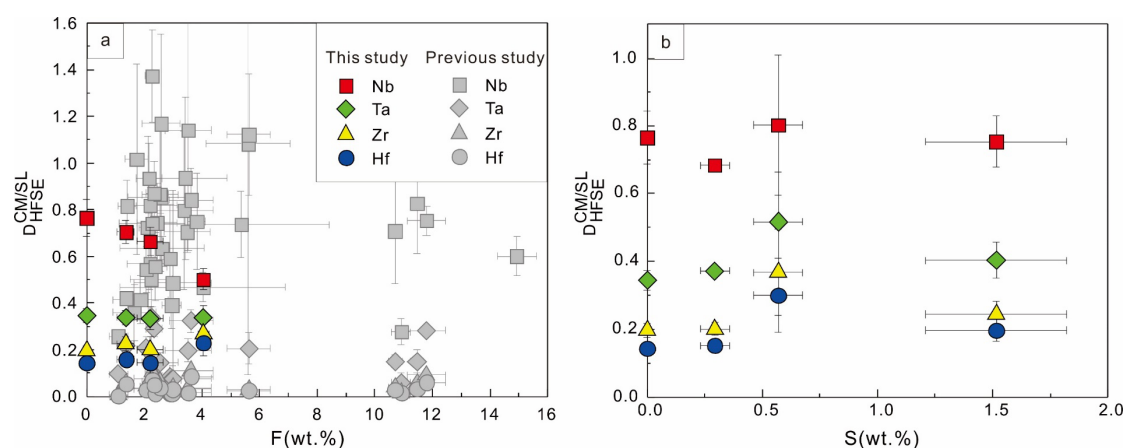
**Supplementary Figure S1. (a) The high-field strength element content characteristics of natural carbonatite samples. PM: primitive mantle, values are from McDonough and Sun (1995). (b) The Nb/Ta and Zr/Hf ratios of natural carbonatites. The gray area represents the Nb/Ta and Zr/Hf ratio characteristics of the silicate end-member rocks commonly found on Earth Pfänder et al. (2007). These data were collected from the GEOROC database.**



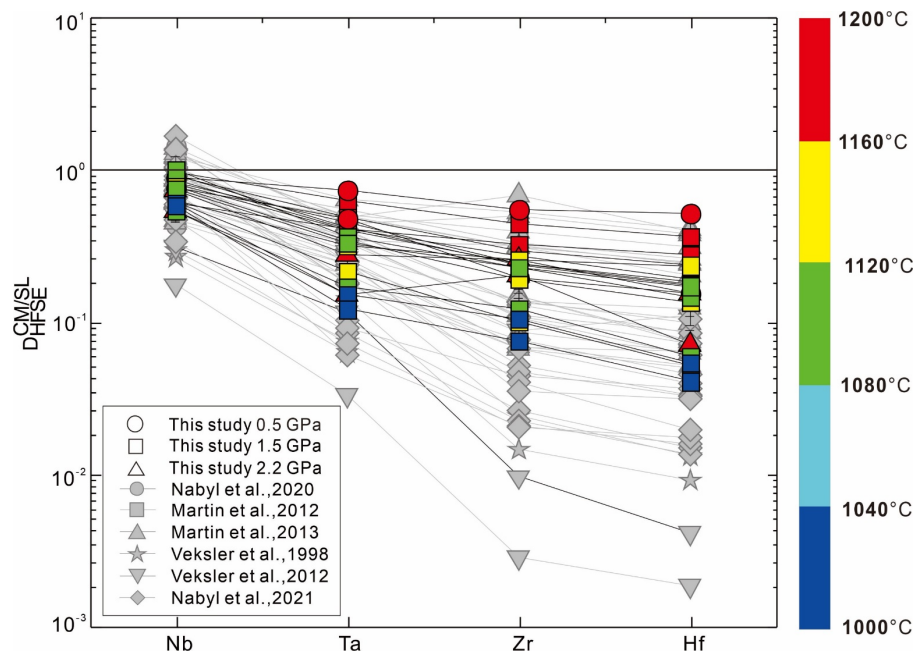
**Supplementary Figure S2. Illustration of the correlation between  $\text{SiO}_2$  content and high-field-strength element content in carbonatite melt. The data comes from this study and previous studies (Martin et al., 2013; Martin et al., 2012; Naby et al., 2021; Naby et al., 2020; Veksler et al., 2012).**



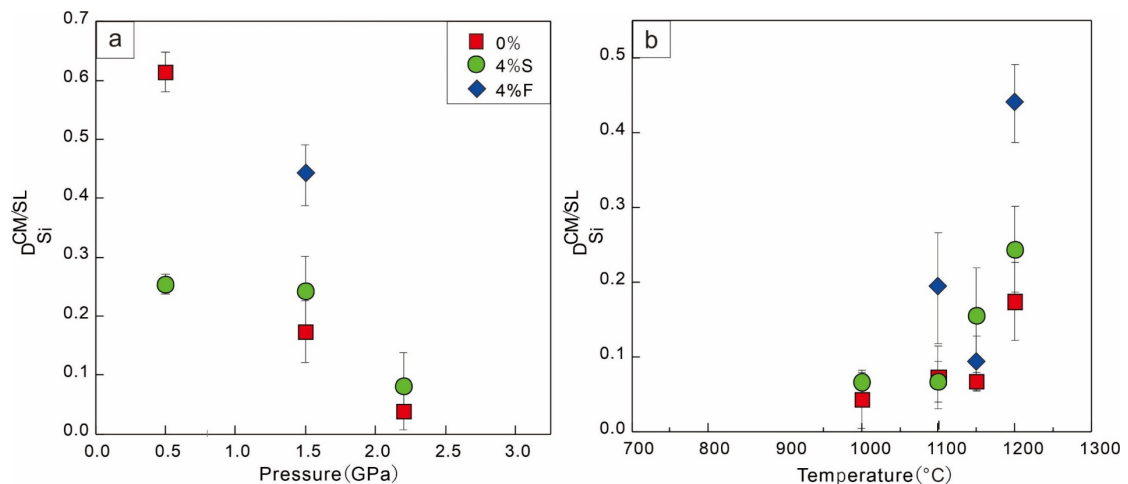
**Supplementary Figure S3. Illustration of the correlation between  $\text{SiO}_2$  content and high-field-strength element content in conjugate silicate melt.** The data comes from this study and previous studies (Martin et al., 2013; Martin et al., 2012; Naby et al., 2021; Naby et al., 2020; Veksler et al., 2012).



**Supplementary Figure S4.  $D_{\text{HFSE}}^{\text{CM/SL}}$  against F (wt. %) in carbonatitic melt (a) and  $\text{SO}_3$  (wt. %) in carbonatitic melt (b).** Noteworthy, no significant correlation between the  $\text{SO}_3$ , F and the  $D_{\text{HFSE}}^{\text{CM/SL}}$  were observed. The data comes from this study and previous studies (Naby et al., 2021; Naby et al., 2020; Veksler et al., 2012).



**Supplementary Figure S5. Comparison of partition coefficients of high field strength elements between carbonatite and conjugate alkaline silicate melts from this study and previous studies.** The carbonatitic melt is represented by CM and the silicate liquid by SL. The data from previous studies are from Veksler et al. (1998, 2012), Martin et al. (2012, 2013), and Naby et al. (2020, 2021). The partition coefficients from this study are consistent with the patterns seen in previous studies, although they are up to one order of magnitude higher than those of Veksler et al. (1998, 2012).



**Supplementary Figure S6. Diagrams illustrating the dependence of  $D_{Si}^{CM/SL}$  on pressure (a) and temperature (b).** As shown, increasing temperature and decreasing pressure both lead to higher values of  $D_{Si}^{CM/SL}$ .

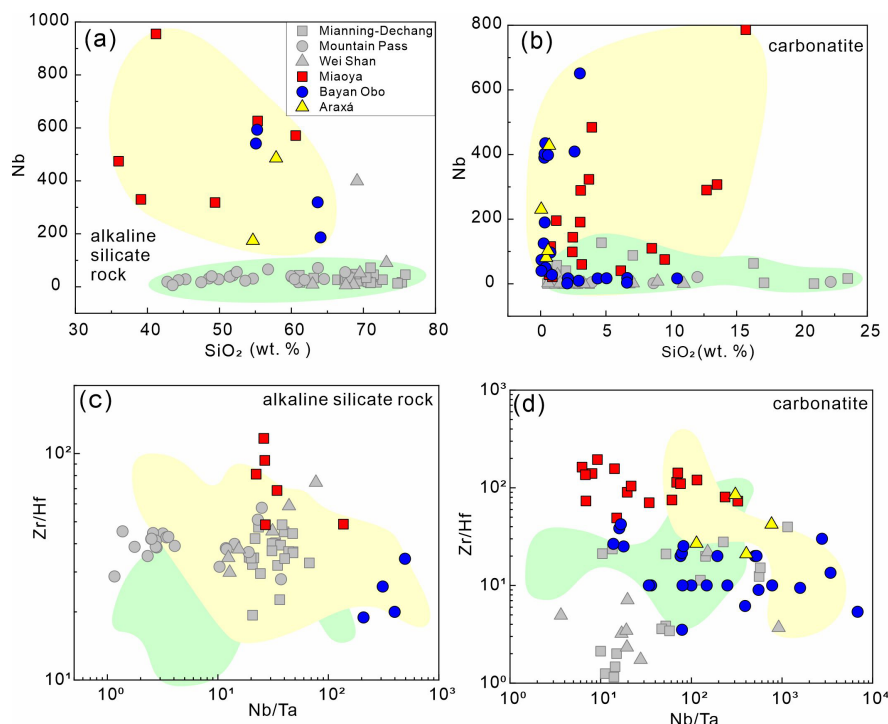


**Figure S7. (a) and (b):** Correlation diagrams show the Nb and SiO<sub>2</sub> from both Nb mineralized and non-mineralized carbonatite-silicate complex. **Panels (c) and (d)** illustrate the Zr/Hf versus Nb/Ta ratios in natural carbonatite-silicate complexes. The carbonatite-silicate complex data is sourced from Weishan (China), Mianning-Dechang Belt (China), Mountain Pass (America), Miaoya (China), Bayan Obo (China), and Araxá (Brazil) (Castor, 2008; Hou et al., 2015; Hou et al., 2006; Liu et al., 2019; Palmieri et al., 2022; Poletti et al., 2016; Su et al., 2019; Verplanck et al., 2016; Wang et al., 2019; Wang et al., 2001; Xu et al., 2003; Yang et al., 2023; Zhang et al., 2019). In these diagrams, colored symbols represent mineralized complexes, while gray symbols represent non-mineralized complexes. Notably, the primitive magma in mineralized systems exhibits higher Nb content than in non-mineralized systems. Additionally, the immiscible silicate melt in mineralized systems has a lower SiO<sub>2</sub> content.

### **Captions for Tables S1 to S3**

**Table S1.** Major and trace elements of the quenched carbonatite melts (major elements in wt.%; trace elements in ppm).

**Table S2.** Major and trace elements of the silicate liquid (in ppm for trace elements and in wt.% for major elements).

**Table S3.** Major and trace elements of the natural carbonatite-silicate complex samples (major elements in wt.%; trace elements in ppm).



## References cited

- Castor, S. (2008) The Mountain Pass rare-earth carbonatite and associated ultrapotassic rocks, California. *Canadian Mineralogist - CAN MINERALOG*, 46, 779-806.
- Dasgupta, R., and Hirschmann, M.M. (2006) Melting in the Earth's deep upper mantle caused by carbon dioxide. *Nature*, 440(7084), 659-662.
- Hou, Z.Q., Liu, Y., Tian, S.H., Yang, Z.M., and Xie, Y.L. (2015) Formation of carbonatite-related giant rare-earth-element deposits by the recycling of marine sediments. *Scientific Reports*, 5(1), 10231.
- Hou, Z.Q., Tian, S.H., Yuan, Z.X., Xie, Y.L., Yin, S.P., Sheng, Y.L., Fei, H.C., and Yang, Z.M. (2006) The Himalayan collision zone carbonatites in western Sichuan, SW China: Petrogenesis, mantle source and tectonic implication. *Earth and Planetary Science Letters*, 244, 234-250.
- Jochum, K.P., and Nohl, U. (2008) Reference materials in geochemistry and environmental research and the GeoReM database. *Chemical Geology*, 253(1-2), 50-53.
- Jochum, K.P., Weis, U., Stoll, B., Kuzmin, D., Yang, Q., Raczek, I., Jacob, D.E., Stracke, A., Birbaum, K., and Frick, D.A. (2011) Determination of reference values for NIST SRM 610-617 glasses following ISO guidelines. *Geostandards Geoanalytical Research*, 35(4), 397-429.
- Lane, S.J., and Dalton, J.A. (1994) Electron microprobe analysis of geological carbonates. *American Mineralogist*, 79(7-8), 745-749.
- Liu, Y., Chakhmouradian, A.R., Hou, Z., Song, W., and Kynický, J. (2019) Development of REE mineralization in the giant Maoniuping deposit (Sichuan, China): insights from mineralogy, fluid inclusions, and trace-element geochemistry. *Mineralium Deposita*, 54(5), 701-718.
- Liu, Y.S., Hu, Z.C., Gao, S., Gunther, D., Xu, J., Gao, C.G., and Chen, H.H. (2008) In situ analysis of major and trace elements of anhydrous minerals by LA-ICP-MS without applying an internal standard. *Chemical Geology*, 257(1-2), 34-43.
- Martin, L.H., Schmidt, M.W., Mattsson, H.B., and Guenther, D. (2013) Element partitioning between immiscible carbonatite and silicate melts for dry and H<sub>2</sub>O-bearing systems at 1-3 GPa. *Journal of Petrology*, 54(11), 2301-2338.
- Martin, L.H., Schmidt, M.W., Mattsson, H.B., Ulmer, P., Hametner, K., and Günther, D. (2012) Element partitioning between immiscible carbonatite-kamafugite melts with application to the Italian ultrapotassic suite. *Chemical Geology*, 320, 96-112.
- McDonough, W.F., and Sun, S.-S. (1995) The composition of the Earth. *Chemical geology*, 120(3), 223-253.
- Nabyl, Z., Gaillard, F., Tuduri, J., and Di Carlo, I.J.C.R.G. (2021) No direct effect of F, Cl and P on REE partitioning between carbonate and alkaline silicate melts. *Comptes Rendus. Géoscience*, 353(S2), 233-272.
- Nabyl, Z., Massuyeau, M., Gaillard, F., Tuduri, J., Iacono-Marziano, G., Rogerie, G., Le Trong, E., Di Carlo, I., Melleton, J., and Bailly, L.J.G.e.C.A. (2020) A window in the course of alkaline magma differentiation conducive to immiscible REE-rich carbonatites. *Geochimica et Cosmochimica Acta*, 282, 297-323.
- Palmieri, M., Brod, J.A., Cordeiro, P., Gaspar, J.C., Barbosa, P.A.R., de Assis, L.C., Junqueira-Brod, T.C., Silva, S.E.e., Milanezi, B.P., Machado, S.A., and Jácomo, M.H. (2022) The Carbonatite-Related Morro do Padre Niobium Deposit, Catalão II Complex, Central Brazil. *Economic Geology*, 117(7), 1497-1520.
- Pearce, N.J., Perkins, W.T., Westgate, J.A., Gorton, M.P., Jackson, S.E., Neal, C.R., and Chenery, S.P.

- (1997) A compilation of new and published major and trace element data for NIST SRM 610 and NIST SRM 612 glass reference materials. *Geostandards newsletter*, 21(1), 115-144.
- Pfänder, J.A., Münker, C., Stracke, A., and Mezger, K. (2007) Nb/Ta and Zr/Hf in ocean island basalts—implications for crust–mantle differentiation and the fate of Niobium. *Earth Planetary Science Letters*, 254(1-2), 158-172.
- Poletti, J.E., Cottle, J.M., Hagen-Peter, G.A., and Lackey, J.S. (2016) Petrochronological Constraints on the Origin of the Mountain Pass Ultrapotassic and Carbonatite Intrusive Suite, California. *Journal of Petrology*, 57(8), 1555-1598.
- Rocholl, A. (1998) Major and trace element composition and homogeneity of microbeam reference material: Basalt glass USGS BCR-2G. *Geostandards newsletter*, 22(1), 33-45.
- Su, J.H., Zhao, X.F., Li, X.C., Hu, W., Chen, M., and Xiong, Y.L. (2019) Geological and Geochemical Characteristics of the Miaoya Syenite-Carbonatite Complex, Central China: Implications for the Origin of REE-Nb-enriched Carbonatite. *Ore Geology Reviews*, 113, 103101.
- Veksler, I.V., Dorfman, A.M., Dulski, P., Kamenetsky, V.S., Danyushevsky, L.V., Jeffries, T., and Dingwell, D.B. (2012) Partitioning of elements between silicate melt and immiscible fluoride, chloride, carbonate, phosphate and sulfate melts, with implications to the origin of natrocarbonatite. *Geochimica et Cosmochimica Acta*, 79, 20-40.
- Verplanck, P.L., Mariano, A.N., Mariano, A., Jr., Verplanck, P.L., and Hitzman, M.W. (2016) Rare Earth Element Ore Geology of Carbonatites. *Rare Earth and Critical Elements in Ore Deposits*, 18, p. 0. Society of Economic Geologists.
- Wang, C., Liu, J.C., Zhang, H.D., Zhang, H.D., Zhang, X.Z., Zhang, D.M., Xi, Z.X., and Wang, Z.J. (2019) Geochronology and mineralogy of the Weishan carbonatite in Shandong province, eastern China. *Geoscience Frontiers*, 10(2), 769-785.
- Wang, D.H., Yang, J.M., Yan, S.H., Xu, J., Chen, Y.C., Pu, G.P., and Luo, Y.N. (2001) A Special Orogenic-type Rare Earth Element Deposit in Maoniuping, Sichuan, China: Geology and Geochemistry. *Resource Geology*, 51, 177-188.
- Xu, C., Huang, Z.L., Liu, C.Q., Qi, L., Li, W.B., and Guan, T. (2003) Geochemistry of carbonatites in Maoniuping REE deposit, Sichuan province, China. *Science in China Series D: Earth Sciences*, 46(3), 246-256.
- Yang, K.F., Fan, H.R., Pirajno, F., and Liu, X. (2023) Magnesium isotope fractionation in differentiation of mafic-alkaline-carbonatitic magma and Fe-P-REE-rich melt at Bayan Obo, China. *Ore Geology Reviews*, 157, 105466.
- Zhang, D.X., Liu, Y., Pan, J.Q., Dai, T., and Bayless, R. (2019) Mineralogical and Geochemical Characteristics of the Miaoya REE Prospect, Qinling Orogenic Belt, China: Insights from Sr-Nd-C-O Isotopes and LA-ICP-MS Mineral Chemistry. *Ore Geology Reviews*, 110.